

# A SYSTEM OF SYSTEMS AIRCRAFT DESIGN FRAMEWORK: DEMONSTRATION USING A SEAPLANE TRANSPORT NETWORK IN THE GREEK ISLANDS

Vincenzo Nugnes<sup>1</sup>, Carmine Varriale<sup>2</sup>, Patrick Ratei<sup>1</sup>, Prajwal Shiva Prakasha<sup>1</sup> & Björn Nagel<sup>1</sup>

<sup>1</sup>German Aerospace Center (DLR), Institute of System Architectures in Aeronautics, Hein-Saß-Weg 22, 21129 Hamburg, Germany

<sup>2</sup>Delft University of Technology, Faculty of Aerospace Engineering, Kluyverweg 1, 2629 HS Delft, Netherlands

#### **Abstract**

This paper presents a System of Systems Engineering approach to aircraft design. For this purpose, conventional design disciplines are coupled with Agent-Based Modeling and Simulation (ABMS) defining a unique optimization problem. The proposed methodology is applied to design seaplanes for an on-demand transportation system connecting the Greek islands. Within this network, diverse scenarios are analyzed by varying parameters of the model such as fleet size and travel demands at each seaport. The objective is to show the impact of including ABMS in the design workflow on the optimized seaplane design parameters. The optimum designs are evaluated on the basis of a number of performance metrics, to assess to what extent they can aid (or substitute) existent maritime means of transportation. The results reveal optimal fleet performance for seaplanes characterized by lower cruise speeds and passenger capacities, as compared to those derived from conventional methodologies and to existing designs.

Keywords: system of systems, conceptual aircraft design, agent-based modeling and simulation, seaplane

### **Nomenclature**

propeller diameter  $D_{\mathsf{prop}}$ **Subscripts** reference value mass re f ṁ mass flow CRcruise  $M_{CR}$ cruise Mach number Ffuel FF $n_{pax}$ passenger capacity fleet fuel array of motors rated powers PTpowertrain  $R_{\mathsf{des}}$ aircraft design range **Superscripts** array of mission velocities initial value requests converted optimal value

#### 1 Introduction

Aircraft design is rapidly advancing through the adoption of new methodologies that enhance the precision and efficiency of analyses and calculations. The integration of innovative powertrain technologies allows researchers to develop more efficient designs, with reduced fuel consumption and emissions. Nevertheless, there remains a notable gap in considering how these aircraft configurations behave in the existing transportation system, which depends on a multitude of interconnected component systems to deliver services [1, 2]. This paper proposes a System of Systems Engineering (SoSE) perspective on aircraft design with the aim of including requirements of the operational environment in the design process [3]. The conceptual aircraft design is tailored to specific scenarios of operation using Agent-Based Modeling and Simulation (ABMS).

A System of Systems (SoS) can be simply defined as any other system: it "consists of parts, relationships and a whole that is greater than the sum of the parts" [4]. However, within a SoS the "parts" are

independent systems themselves, and a majority of the following characteristics are present: operational and managerial independence, geographic distribution, emergent behavior, and evolutionary development [5].

ABMS is believed to be one of the most suited techniques to model a SoS, in particular for transportation [6]. It is defined as "a computational method that enables a researcher to create, analyze, and experiment with models composed of agents that interact within an environment" [7]. More particularly, ABMS holds the potential for capturing the interactions among various stakeholders in transportation, such as airlines, air traffic control, passengers, and policymakers [7]. It also allows for the modeling and investigation of uncertainties related to travel demands, resource availability, and/or operational procedures that might be present in the system [8]. One relevant example of using ABMS to model a transportation system is provided by Prakasha et al. [2], who showed the importance of considering other systems than the aircraft to determine the latter's effectiveness in fleet operations. In a similar way, this paper introduces an aircraft design optimization process that is driven by an overall scenario analysis. For this purpose, conventional design disciplines are coupled with ABMS, defining a unique aircraft design optimization problem. To validate this methodology, we propose a proof of concept design framework in which the design of a seaplane is driven by the performance of a fleet operating in an on-demand transportation system serving the Greek islands.

Seaplanes have been considered in the study due to the recent interest researchers have shown in this configuration. Seaplanes played an important role in the aviation industry during the first half of the past century. Due to their ability to take-off and land on water bodies, these aircraft were widely employed in military operations as well as passenger transportation. However, as numerous runways were built worldwide during and after World War II, the relevance of seaplanes waned [9]. In recent times, a renewed interest in these vehicles has emerged. Nevertheless, contemporary contributions fail to implement modern design approaches and lack a holistic view of the transport system in the design process, as seen for aircraft design [10, 11, 12].

The proof of concept framework proposed in this paper has a dual purpose: on the one hand, it shows the impact of including ABMS in the aircraft design workflow, and on the other, it demonstrates the potential of seaplanes as an alternative mode of transportation. The first goal is achieved by investigating the sensitivity of the optimized seaplane design parameters with respect to scenario parameters such as fleet size and travel demands at each seaport. The results of the framework are compared to conventionally designed seaplanes to establish the significance of the new approach. Secondly, in order to assess the effectiveness of seaplanes in enhancing the connections among Greek islands, several analyses are performed to estimate the average travel time, fuel efficiency, CO<sub>2</sub> emissions, and percentage of travellers choosing to fly on seaplanes in different conditions (scenarios). Finally, the design requirements for seaplanes to improve the transport quality in the islands' network are identified.

The paper is structured as follows: in the next section, the SoS design framework is introduced. The proof of concept used to demonstrate it, and the tools composing it, are illustrated in the same section. There, some space is also dedicated to explaining the development needed to adapt these tools into the framework. In Section 3, the scenarios modelled in the ABMS, and the assumptions they are based upon, are specified. The results are shown in Section 4. Finally, the conclusion can be found in Section 5.

## 2 Methodology

Fig. 1 depicts a flowchart representation of the methodology and it shows how the composing blocks are connected together. At the start of an optimization, a set of predefined Top Level Aircraft Requirements (TLARs) is input in the aircraft design block of the framework. The main goal for this first part is to design the vehicle that will be simulated in the ABMS. The design can be performed at any level of fidelity as long as the input requirements for the ABMS are met. The aircraft design tool palette outputs the mission performance of the vehicle which can be used to evaluate the energy consumption and the travel time in the ABMS.

ABMS is then used to simulate the operation of a homogeneous fleet constituted by instances of the aircraft designed in the previous step. The environment of operation is a fixed scenario characterized by a certain demand distribution and a network of nodes to be connected by the above-mentioned

fleet. The fidelity used to represent the scenario in the ABMS, and the assumptions adopted, play a pivotal role in the reliability of the design framework. The results of the simulation will then drive the choice of a new set of TLARs. The process is iterated until an optimum design, according to set criteria, is found.

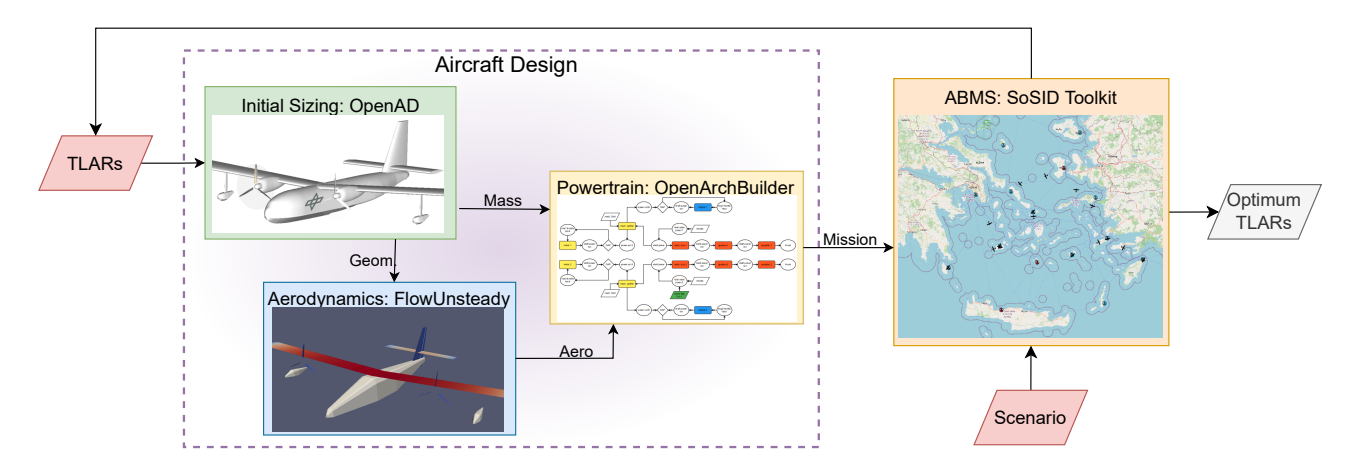


Figure 1 – System of Systems aircraft design framework flowchart

# 2.1 System of Systems seaplane design framework

The proof of concept encompasses a seaplane design framework where the aircraft is assessed within an on-demand transportation system connecting the Greek islands.

The seaplane design is kept at a conceptual stage to mitigate computational costs, and it is performed in three phases, as shown in the dashed box in Fig. 1. First, the entire vehicle is sized with the overall aircraft sizing tool OpenAD (OAD) [13]. The design is then refined with two additional tools: FlowUnsteady [14], to obtain a physics-based calculation of the drag polar of the vehicle, and OpenArchBuilder (OAB) [15], which retrofits a hybrid-electric powertrain on the initial design provided by OpenAD.

OpenAD is a software platform for conceptual aircraft design and sizing developed by DLR. It is based on publicly available textbook methods and DLR custom methods. It is used for seaplane geometry and mass sizing, and to provide an initial estimation of engine performance, aerodynamic polar, and mission analysis.

FlowUnsteady is an open-source solver based on the reformulated vortex particle method (rVPM). It is used to re-calculate the aerodynamic polar of the seaplane. The analyses are performed for cruise speed only, assuming the polar stays unchanged at climb and descent speeds. The vehicle is set in clean configuration and the solver to quasi-steady assumptions, allowing for a low computational effort, and better complements the geometry design fidelity (low). The steps taken to adapt the tool for seaplane geometries are described in Section 2.3.1

OpenArchBuilder is a tool for electric propulsion systems conceptual design. It makes use of the open source tool openconcept [16], and OpenAD, to optimize the propulsion system components and perform mission analysis. It is employed within this framework to retrofit a hybrid-electric powertrain on the seaplane as sized by OpenAD, and to re-calculate its fuel flow rate in the different mission phases. This process was already successfully performed by Bussemaker et al. [17]. The changes introduced to fit the tool in the methodology can be found in Section 2.3.2.

Lastly, the SoS Inverse Design (SoSID) Toolkit [18] (also referred to as Toolkit) is an agent-based model developed by DLR to simulate Urban Air Mobility (UAM) networks connected by fully electric vertical take-off and landing vehicles, and cars. In particular, it allows for the simulation of an ondemand transportation system over a predefined network of nodes and for a set demand distribution. The model has been adapted for the simulation of seaplanes and ferry fleets using a new agent performance model. This process is described in section 2.3.3. The Toolkit provides reports of all flight segments performed during one day of operation. These are used in the framework to obtain values of fleet and aircraft fuel consumption, flight time, passengers transported, and number of

missions performed. Moreover, three main types of uncertainties in fleet operation are modeled in the Toolkit: resources, timing, and demand uncertainties. In Section 3, one uncertainty parameter for each category is selected and varied to investigate their impact on the outputs of the framework. The results of this sensitivity analysis are shown in Section 4.

All tools presented above are connected and executed in the Remote Component Environment (RCE) platform [19], the DLR open-source integration environment. The Common Parametric Aircraft Configuration Schema (CPACS) [20], the open-source data format created by DLR, is used to guarantee standardization of tools inputs and outputs. The formal description of the optimization problem introduced above is provided in the next section.

## 2.2 Optimization problem set up

The eXtended Design Structure Matrix (XDSM) shown in Fig. 2 depicts the type and logic of information exchanged by the tools. An initial guess of the design vector (Eq. 1) is provided to the optimizer to start the optimization loop. The optimizer feeds the design variables to OpenAD, which performs an initial sizing of the seaplane. OpenAD forwards the aircraft geometry to FlowUnsteady, which analyzes the vehicle aerodynamics. Masses, geometry, and performance estimated by OpenAD, and the aerodynamic polar calculated by FlowUnsteady, are used in OpenArchBuilder to start a nested optimization loop, where the components of a hybrid electric powertrain are sized. Within this loop, an hybrid electric propulsion system is retrofitted on the seaplane designed by OpenAD, and masses and design mission are recalculated. At this point, the Maximum Take-Off Mass (MTOM) of the seaplane is compared to the initial estimation provided by OpenAD to check the consistency of the design (constraint in Eq. 2). The aircraft thus designed is provided as input to the SoSID Toolkit, together with the scenario of operation. The seaplane fleet operation is then simulated. Finally, the objective function (Eq. 3) is evaluated from the outputs of the ABMS. The objective value is fed back to the optimizer, which will then restart the loop with an updated design vector. The process is iterated until an optimum is found. The scenario is a constant input of the optimization loop, and it is defined in Section 3. The boxes on the leftmost column represent the optimal values that will be the final output of the optimization.

$$\vec{x} = [n_{pax}, M_{CR}, R_{DES}] \tag{1}$$

$$0.8 \cdot MTOM_{OAD} \le MTOM_{OAB} \le 1.2 \cdot MTOM_{OAD} \tag{2}$$

$$f = \frac{m_{FF}}{m_{FF-ref}} - \frac{\lambda}{\lambda_{ref}} \tag{3}$$

The design variables of this problem are: cruise Mach number, payload mass (expressed as passenger capacity), and design range of the aircraft (Eq. 1). Their choice was driven by the characteristics of the available design tools and by the fact that these aircraft parameters are also direct inputs of the ABMS. The objective function is a mixed objective that aims to minimise fleet fuel consumption while maximising the converted passengers' requests (the percentage of passengers choosing to travel with seaplanes) during one day of operation (Eq. 3). The problem is constrained to the bounds listed in Eq. 4. The bounds for the number of passengers are dictated by the choice of designing a seaplane in the CS23 class. The minimum cruise Mach number is imposed by OpenArchBuilder, while the maximum is defined according to values for aircraft in the CS23 class. The bounds for the design range are set to be the distance between the two furthest apart neighboring islands and the maximum distance between any two islands in the network. The latter is clarified in Section 3, where the islands' network is introduced.

$$6 \le n_{pax} \le 19$$
  
 $0.20 \le M_{CR} \le 0.30$  (4)  
 $140 \le R_{DES} \le 500km$ 

Due to the nature of the optimization problem, where the gradient of the objective function is unknown, the optimizer selected for this optimisation is NOMAD, developed by Le Digabel [21] based on the Mesh Adaptive Direct Search (MADS) algorithm. NOMAD is designed for black-box optimization, where the objective function is a costly program, with no derivative information, and where some evaluations may return no values. In fact, NOMAD minimizes the number of evaluations needed to find the optimal solution and can handle discrete variables.

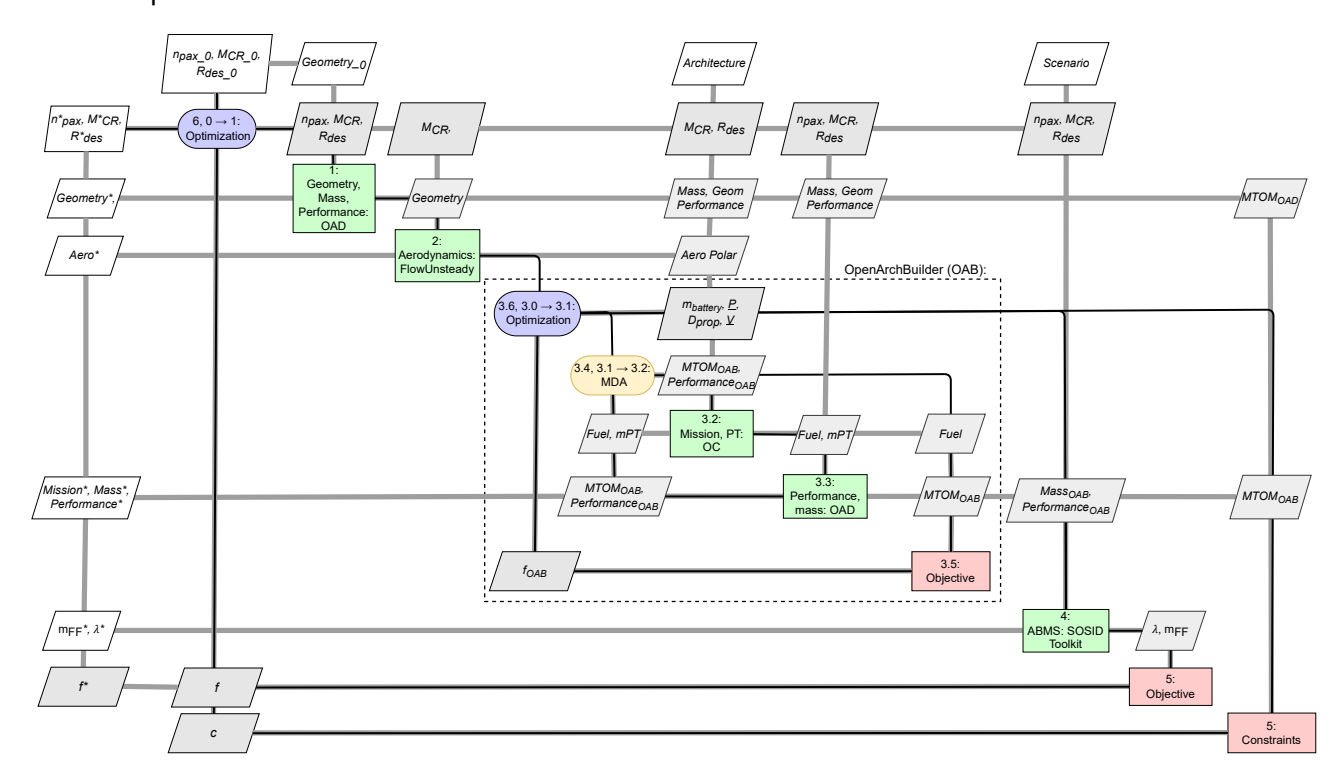


Figure 2 – XDSM diagram of the System of Systems aircraft design optimization problem

# 2.3 Tools development and adaptation to the framework

The most important modifications applied to the tools to make sure they could handle seaplane-specific data are explained in the following sections. All tools in the framework communicate with each other thanks to pre-processing scripts created for each tool to read CPACS files in input. In the same way, post-processing scripts were created to convert outputs into CPACS files that could be interpreted as input by the following tool.

## 2.3.1 FlowUnsteady

FlowUnsteady offers a set of pre-built functions to describe wing and propeller geometries and to perform custom aerodynamics analyses. To represent a full seaplane, a function to define hull-shaped fuselages and tip-float components was introduced. This custom function takes the components' dimensions and cross-section as input from OpenAD, and it produces a loft surface over a sweep of seven cross-sections opportunely scaled.

The tool considers fuselage and tip-floats in the flow field but does not compute aerodynamic forces on them. The drag caused by these components is estimated in OpenAD with a semi-empirical method [22], and added to the total drag at each point of the polar.

# 2.3.2 OpenArchBuilder

The tool is used to set up a second (nested) optimization loop at the vehicle level which aims to size the hybrid-electric powertrain components, most importantly the battery, and to calculate the seaplane mission performance, as shown in Fig. 2. In this application, the input powertrain architecture is fixed to a parallel hybrid-electric configuration. The choice is based on the fact that this configuration performs better in terms of weight and fuel consumption over a wide range of degrees of hybridization [15, 17].

To adapt the tool to the framework, the cruise horizontal speed is fixed at the value dictated by the design variable  $M_{CR}$  passed by the main loop optimizer. The vertical speed at cruise is set to zero to ensure cruise at constant altitude. The Degree of Hybridization (DoH) with respect to power is considered to be zero during descent and the entire reserve segment [23], while optimized for climb and cruise. Thus,  $DoH_{CR}$  and  $DoH_{climb}$  were added to the design vector [15]. The objective function aims to minimize MTOM and fuel mass [15].

The battery pack specifications chosen by Fouda et al. [15] were considered to be too optimistic for a 2030+ time frame. Thus, Li-ion batteries with a specific power of 1 kW/kg and a specific energy of 350 Wh/kg were considered instead [24, 23, 25, 26]. The most relevant assumptions are listed in Table 1.

Table 1 –	Technological	assumptions	for pov	vertrain :	sizina

Component	Specific Power (kW/kg)	Efficiency (%)	PSFC lb/(hp/h)
Battery	1	97	-
Motor	5	97	-
Generator	5	97	-
Converter	10	97	-
Turboshaft	7.15	=	0.6
Bus	-	95	-

# 2.3.3 SoSID Toolkit

The aircraft agents' behavior was adapted for the simulation of seaplanes by implementing a mission profile including taxi, take-off, climb, cruise, descent, loiter, and landing phases. Moreover, the agent performance model used to monitor the aircraft energy consumption has been updated in the following way. Taxi, take-off, and landing fuel consumption are considered constant. These values are estimated once for every seaplane in the aircraft design block of the framework. In the ABMS, seaplanes are required to fly a variety of missions often differing from the design one, therefore mission performance (for climb, cruise, and descent phases) are actively modeled in the simulation. In particular, fuel consumption during climb, cruise, and descent are calculated at every time step starting from the values of fuel mass flow for the design mission. The aircraft mass is updated at every time step by subtracting the instantaneous fuel consumption.

In Fig. 3, fuel mass flow against mass is plotted for the design mission and a representative simulated mission of a placeholder seaplane design. Note that OpenArchBuilder assumes linear dependency between the two quantities during each flight phase. The fuel mass flow for the simulated mission climb phase is obtained by linear translation, starting from the line representing the design mission climb phase. This is achieved by employing Eq. 5, which describes a grid of parallel lines.

$$y = ax + qk \tag{5}$$

Where a is the slope and q is the y-intercept of the design mission climb line. k is a constant that determines the spacing between the two lines and it is defined for each simulated mission as a function of the Take-Off Mass (TOM) (Eq. 6).

$$k = \frac{\dot{m}_F^0 - a \cdot TOM}{q} \tag{6}$$

Where  $\dot{m}_F^0$  is the design mission initial fuel mass flow value.

The fuel mass flow during cruise is assumed to vary linearly across different missions. Therefore, the fuel mass flow for the simulated cruise is obtained directly from the line equation describing the cruise phase of the design mission. The loiter phase is considered a continuation of cruise and is thus modelled in the same way. Finally, the fuel mass flow during descent for the simulated mission is obtained in an analogous way as for the climb phase.

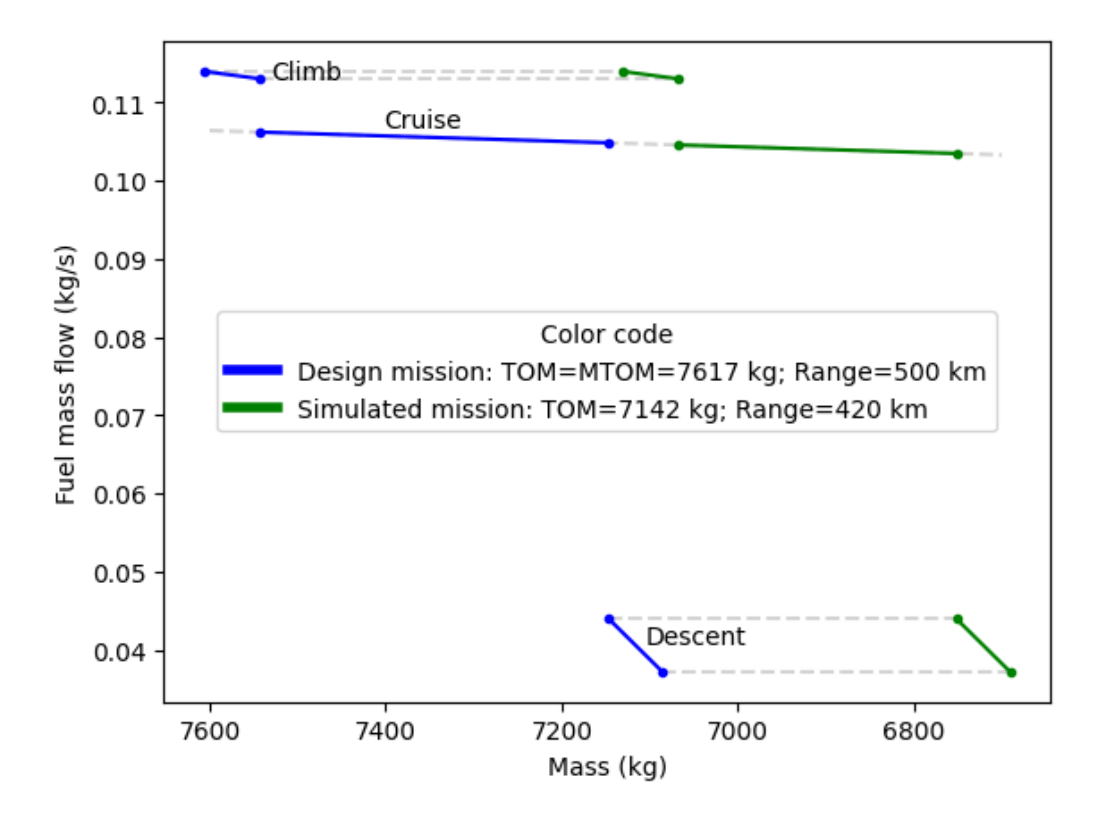


Figure 3 – Aircraft agents performance modeling, design mission and a representative simulated mission of a placeholder seaplane design

One of the objectives of this work is to evaluate to what extent seaplanes can represent a competitive alternative to existing maritime means of transportation in the Greek islands. For this reason, ferry connections have been modelled in the SoSID Toolkit. An average ferry for such an operation was selected [27], and its main features are summarized in Table 2. A fixed schedule, with departure and arrival times to the ports considered was assembled on the basis of information from the main service providers in the Aegean Sea (gathered on Ferryhopper<sup>1</sup>, Seajets<sup>2</sup>, and Blue Star Ferries<sup>3</sup> websites). For every travel request, the Toolkit reads direct routes from the schedule, and it computes possible connecting routes by considering a stopover in each of the other islands in the network. A maximum of one stop is allowed. The earliest possible arrival time by ferry is thus computed. The latter, together with the estimated arrival time by seaplane, is provided to the traveler, who will choose the fastest mode of transportation. (For information regarding the Toolkit models and logic please refer to Kilkis et al. [18]).

The above-mentioned islands network, as well as further assumptions posed for the simulation scenario definition, are described in the following section.

Table 2 – Ferry assumptions

Parameter	Assumed value
Pax capacity	250
Fuel consumption	$658.76\mathrm{kg/h}$

### 3 Scenario definition and assumptions

The input scenario is a network composed of 15 islands and the port of Athens, the Piraeus (Fig. 4). The choice of these seaports stems from the study carried out by Ilopoulou et al. [28], where the

<sup>1</sup>https://www.ferryhopper.com/en/ accessed on 10/2023

<sup>&</sup>lt;sup>2</sup>https://www.seajets.com/ accessed on 10/2023

<sup>3</sup>https://www.bluestarferries.com/en-qb accessed on 10/2023

authors selected 31 islands and identified the most important travel routes in the Aegean. However, in this paper, we reduced the number of ports to 16 to ease the computational power required by the simulation. The iterative selection process discarded the island with the shortest distance to its neighboring one until a set of 16 was obtained. "Neighboring islands" are any two islands directly adjacent, for which the distance between each other is the minimum among all pairs they can form with other islands. It is important to highlight the maximum distance among all neighboring islands as the minimum distance a seaplane should be able to fly to make sure no islands are unreachable. Data from the Hellenic Statistical Authority ELSTAT <sup>4</sup> was used to model the travel requests (demand distribution) in the network. This data, reporting the total number of passengers embarking and disembarking in each of the selected ports every 4 months, allows for the estimation of an average amount of travelers per day. The demand was assumed to be normally distributed throughout the day.

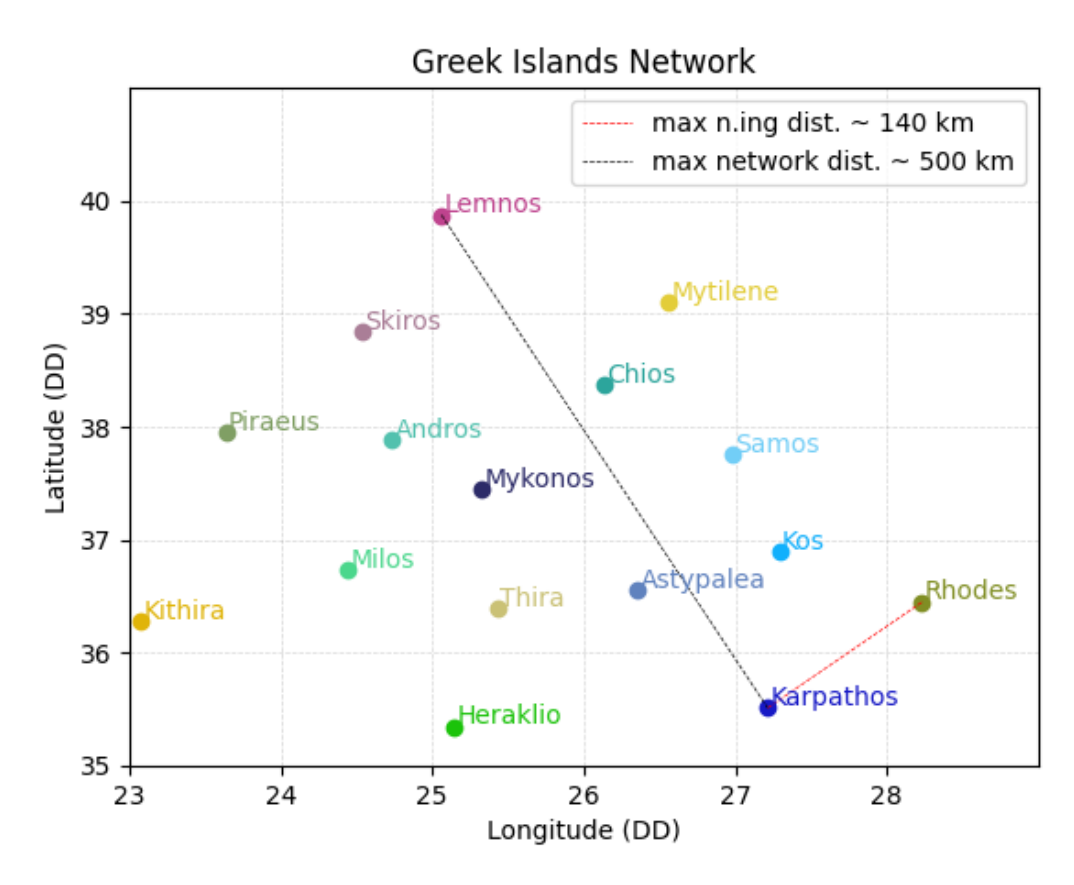


Figure 4 – Greek islands network representation

In order to investigate the effects of resources, timing, and demand uncertainties in the simulation on the outputs of the framework, the fleet size, grouping time window, and demand volume parameters are used to perform a Design of Experiments (DoE). Three fleet sizes are considered in the study: 16, 32, and 48 aircraft. The grouping time window (gw) is the time period during which the aircraft expects additional travel requests (after the first one) to be grouped together for a joint departure. For example, if there is a travel request at time T, the aircraft will wait for additional travel requests until time T+gw before departing. One short and one long grouping windows are considered: 15 and 60 minutes, respectively. Lastly, two travel demand cases are analyzed. The first one considers a low demand case which is representative of the winter season, modelled with data from the first quarter of 2023. The second case considers data collected for the second quarter of 2022, representative of the summer season. With these values, a full factorial DoE was defined, for a total of 12 scenarios (Table 3).

More uncertainty parameters modeled in the Toolkit are listed in Table 4, and are fixed on the basis of the following assumptions. The seaport size is limited to one runway, and the fleet is split into an

<sup>4</sup>https://www.statistics.gr/en/statistics/ind accessed on 10/2023

Table 3 – Summary of all scenarios considered in the study

	Summer					Winter						
Scenario	S.1.1	S.1.2	S.2.1	S.2.2	S.3.1	S.3.2	W.1.1	W.1.2	W.2.1	W.2.2	W.3.1	W.3.2
Demand $(\frac{n_{pax}}{day})$	≈ 3000						≈ 880					
Fleet size (-)	16 32 48		8	16		32		48				
gw (min)	15	60	15	60	15	60	15	60	15	60	15	60

equal number of aircraft among the ports at the beginning of each simulation. The turnaround time was broken down into three components: boarding, disembarking, and deployment time. A total time of 15 minutes is applied to all flights in the simulation independently of the number of passengers [1, 29, 30].

Table 4 – Uncertainties parameters assumptions

Parameter	Assumed value		
Battery specific energy	350 kW h/kg		
Battery specific power	$1 \mathrm{kW/kg}$		
Charging power	$450\mathrm{kW}$		
Seaport size	1 runway		
Turnaround time	15 min		
Refueling rate	$7.7 \mathrm{L/s}$		

This time also includes battery recharging and refueling. Indeed, considering a recharging power of  $450\,\mathrm{kW}$  [31], with the relatively small battery size noted in the design phase (maximally  $300\,\mathrm{kg}$ ), the battery can be fully recharged in maximally 15 minutes. In addition, assuming that the seaports are equipped with a pressure pump, the refueling rate is conservatively estimated to be  $7.7\,\mathrm{L/s}$  [32, 33]. At this rate, seaplanes with tank capacity up to  $7000\,\mathrm{L}$  can be refilled in  $15\,\mathrm{min}$ . A similar study performed on UAM showed that the turnaround time does not have a significant impact on the simulation results [34]. Lastly, taxi time and fuel consumption were also considered to be fixed for each simulation. The values are estimated by OpenAD at every iteration and kept constant during each Toolkit run.

#### 4 Results

Aircraft design problems and ABMS are recognized as challenging to validate. In the context of SoS, theory and experimentation are intertwined within the simulation itself, thereby complicating the validation of results [7]. The tools used to build the proof of concept are singularly validated ([13, 14, 15, 18]). In addition, OpenAD was calibrated by reproducing the flying-boat Canadair CL-415, the successful calibration was then verified by reproducing the flying-boat Sikorsky S-43<sup>5</sup> starting from its passenger capacity, design range and cruise Mach number (Tab. 5). Nevertheless, the analysis and sensitivity study presented in this section play a pivotal role in the framework validation process. Twelve optimizations were performed on the basis of the scenarios set up in Section 3. The outcomes are shown in the following sections. The impact of introducing ABMS in the aircraft design framework on the design variables values (TLARs) is discussed in Section 4.1. The sensitivity of the design variables to changes in the simulation scenario is studied in Section 4.2. In Section 4.3, seaplanes are assessed as a potential innovative mode of transportation in comparison to maritime connections in the Greek islands.

The results of the simulations performed in this paper are represented in blue for winter scenarios and red for summer scenarios. The notations "W.x.y" and "S.x.y" are used to identify both scenarios and seaplanes designed for the corresponding scenario. For example: scenario W.1.1 refers to the first use-case described in Table 3, and seaplane W.1.1 refers to the seaplane designed with the ABMS-driven methodology for scenario W.1.1.

<sup>&</sup>lt;sup>5</sup>https://www.militaryfactory.com accessed on 05/2024

	Aircraft Parameter	Sikorsky S-43	Sikorsky S-43 OAD
	$M_{CR}$ (-)	0.27	0.27
Input	$n_{pax}$ (-)	19	19
<u>=</u>	$R_{DES}$ (km)	1247.00	1247.00
	MTOM (kg)	8845.00	8914.85
Se	MEM (kg)	5783.00	5240.20
Masses	Fuel (kg)	-	1415.75
∑a	Floats (kg)	-	83.77
	Hull (kg)	-	159.52
Ξ.	Length (m)	15.60	22.41
Geom.	Wing span (m)	26.21	25.49
ထိ	Wing area (m <sup>2</sup> )	72.52	72.13

Table 5 – Sikorsky S-43, comparison of OpenAD output and aircraft specifics

# 4.1 Impact of ABMS on seaplane design parameters

To investigate the potential of the newly introduced design methodology, and the effects of adding ABMS in an aircraft design process, the seaplanes designed using the SoS-driven design framework are compared to "concentionally" designed seaplanes.

In Fig. 5, seaplanes W.1.1 and S.1.1 are compared to seaplanes designed with the same aircraft design tools, yet with design choices driven by a standard approach, rather than ABMS. In other words, the TLARs were not output of the SoS-driven optimization, but were deliberately selected according to the following methodologies. The design approach proposed by Patterson et al. [35] was adopted to size seaplane "C1". The design range was set to the maximum distance in the network, and passenger capacity to the maximum for the CS23 class (19 seats), while the cruise speed was sized by OpenAD. The TLARs of design "C2" were chosen by aligning them with those of existing innovative concepts, such as the Viceroy by REGENT<sup>6</sup>. C1 and C2 are represented in yellow and green, respectively. Note that the values in Fig. 5c are dimensionless, they are scaled by the values of the top bounds introduced in Section 2.2.

From Fig. 5, it appears that seaplanes C1 and C2 are oversized with respect to the designs outputted by the SoS-driven framework (W.1.1 and S.1.1). According to the simulation results, the number of seats needed in scenarios W.1.1 and S.1.1 is approximately half of the estimated one for C2 and a third of C1 (6 and 7 against 12 and 19, respectively). As a consequence, the design MTOM is lower, which coupled with the fact that the aircraft fly at a lower cruise speed, provides noticeable savings in fuel consumption.

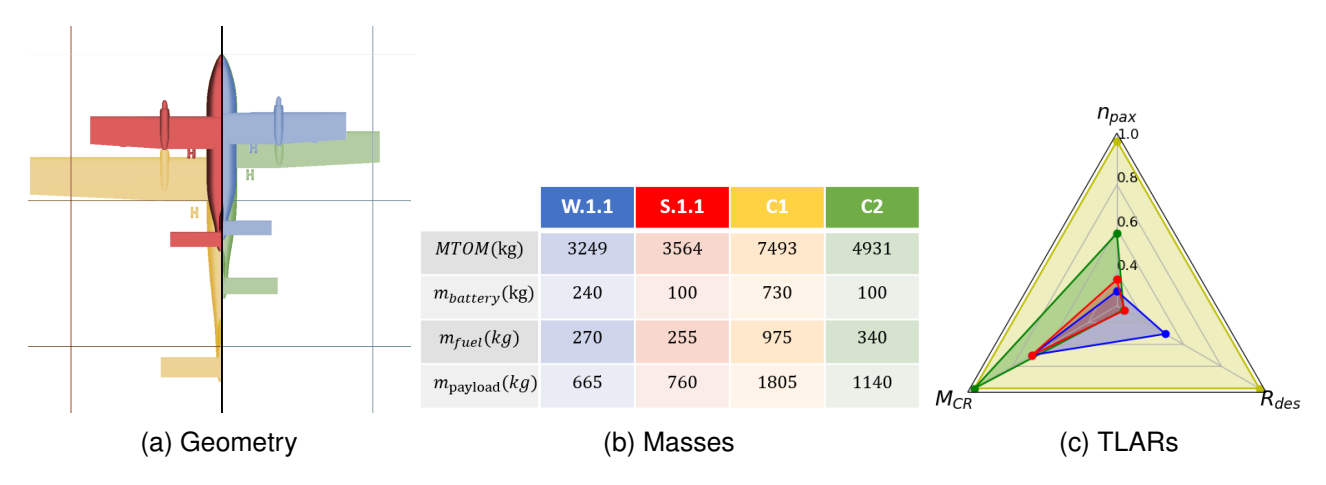


Figure 5 – Comparison of seaplane designs W.1.1, S.1.1, C1, C2

<sup>6</sup>https://www.regentcraft.com/seagliders/viceroy accessed on 11/2023

To give an overview of the performance of the conventional designs against the optimized ones, the fuel consumed and requests converted by each fleet in the different scenarios are compared in Fig. 6. For this, and all subsequent plots the color code introduced above is maintained. Moreover, two different line styles are adopted to distinguish scenarios characterized by grouping time windows of  $15 \, \mathrm{min}$  and  $60 \, \mathrm{min}$ .

Conventional design C1 obtains the highest number of requests converted in every scenario thanks to the high cruise speed, and long range. However, C1 is also the seaplane consuming by far the most fuel, with a fleet fuel consumption over three times larger than the optimized seaplanes (in the best case). Seaplane C2 performs poorly both in terms of fleet fuel consumption and requests converted across all scenarios. Considering both metrics at the same time (the value of the objective function introduced earlier), all seaplanes designed with the newly introduced methodology score better than the conventional designs.

When comparing the performance of the SoS-optimized seaplanes in the different scenarios, almost linear trends are identified for both fleet fuel and requests converted against fleet size. On the other hand, the higher grouping window causes a loss of converted travel requests in the majority of scenarios. This is due to the fact that the higher grouping window is slowing down the seaplane service, thus more passengers prefer the ferries service. By looking at the performance of the optimized fleets in summer against winter scenarios, it emerges that fleet fuel consumption grows with fleet size at similar rates. Contrary, the request converted increase with a steeper angle in winter than in summer.

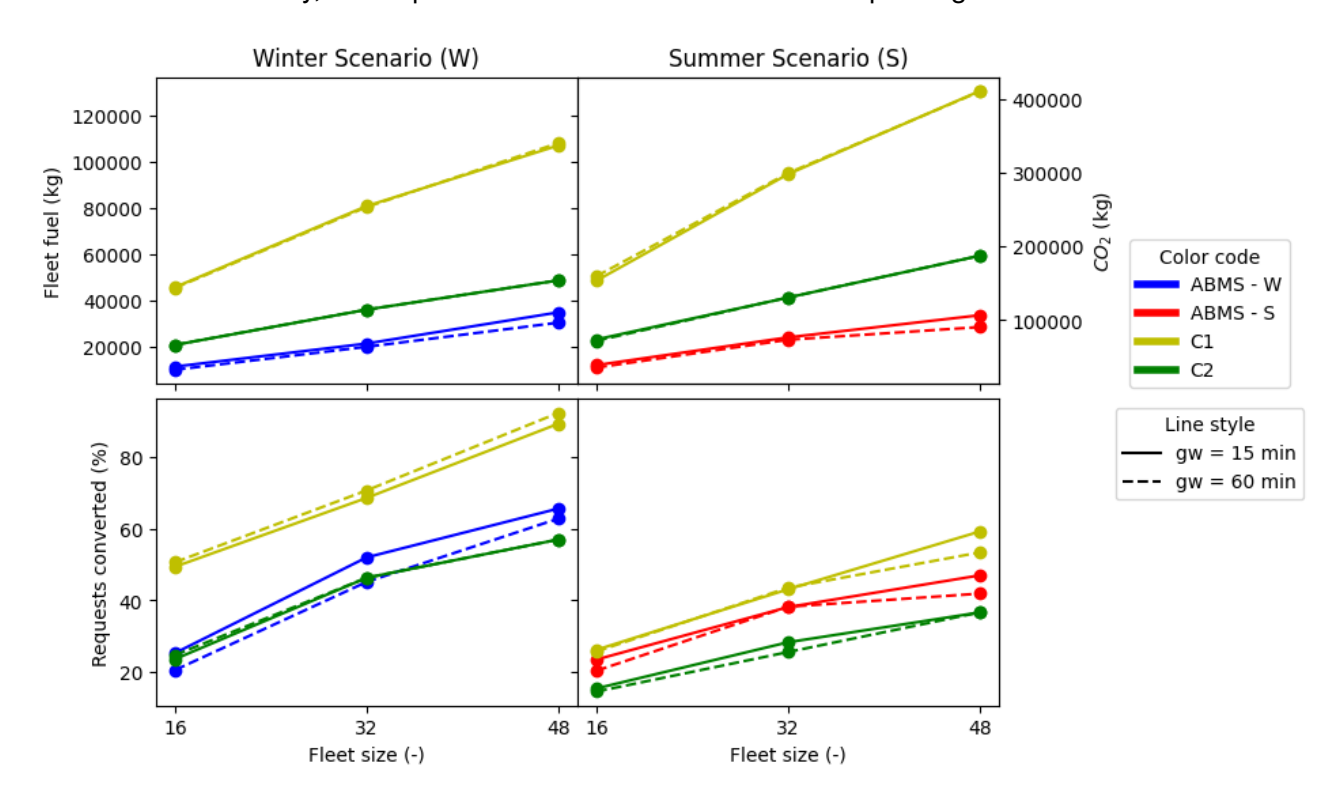


Figure 6 – Fleet performance of conventional designs against ABMS-optimized seaplanes in the different scenarios

# 4.2 Sensitivity of seaplane design variables to scenario parameters

The sensitivity of seaplane design parameters to scenario parameters is investigated in this section. Fig. 7 illustrates the results of the twelve optimization performed. This figure brings light on the variations in optimal TLARs across the different scenarios.

In winter scenarios, the optimum design range registers a drop for fleet size 32. While, the high grouping window ( $gw = 60 \,\mathrm{min}$ ) causes the design range to be consistently lower with respect to the values registered for  $gw = 15 \,\mathrm{min}$ . The optimum cruise Mach number grows with fleet size for  $gw = 60 \,\mathrm{min}$ , and it drops for fleet size 48 when  $gw = 15 \,\mathrm{min}$ . The higher grouping time window determines higher cruise speeds in most cases. Regarding optimum passenger capacity, contrary

to expectations, high gw results in a lower number of seats. This seems correlated to the requests converted for the two grouping windows: fewer passengers are served by seaplanes with smaller capacities.

In summer scenarios, the optimum design parameters seems to be less dependent on fleet size and grouping time window. The design range remains relatively stable with only minor variations as the fleet size increases. There is an initial increase in the cruise Mach number from fleet size 16 to 32, followed by a slight decrease or stabilization from 32 to 48. The trends for different grouping windows show only minor deviations. The variation in passengers capacity is also minimum across the different scenarios, stabilizing around 7.

Comparing the winter and summer scenarios, the optimum design range and cruise Mach number are in general higher in winter, while as expected, the opposite is true for passenger capacity. The winter season shows more variability in optimum design parameters compared to the summer, indicating weaker dependencies of the seaplanes TLARs on scenario parameters with growing demand. Overall, the optimum design vector is found close to the lower bounds of the design domain for all scenarios considered. Low values of design range, cruise Mach number, and passenger capacity are a consequence of the optimization enforcing a reduction in fuel consumption. In addition, this implies that minimizing the fuel consumption outweighs maximizing the requests converted in the scope of minimizing the objective function f. Finally, fleet size 32 appears to be a critical point for all parameters in both seasons, suggesting a balance between operational efficiency and design constraints, however, more data points would be needed to further establish this insight.

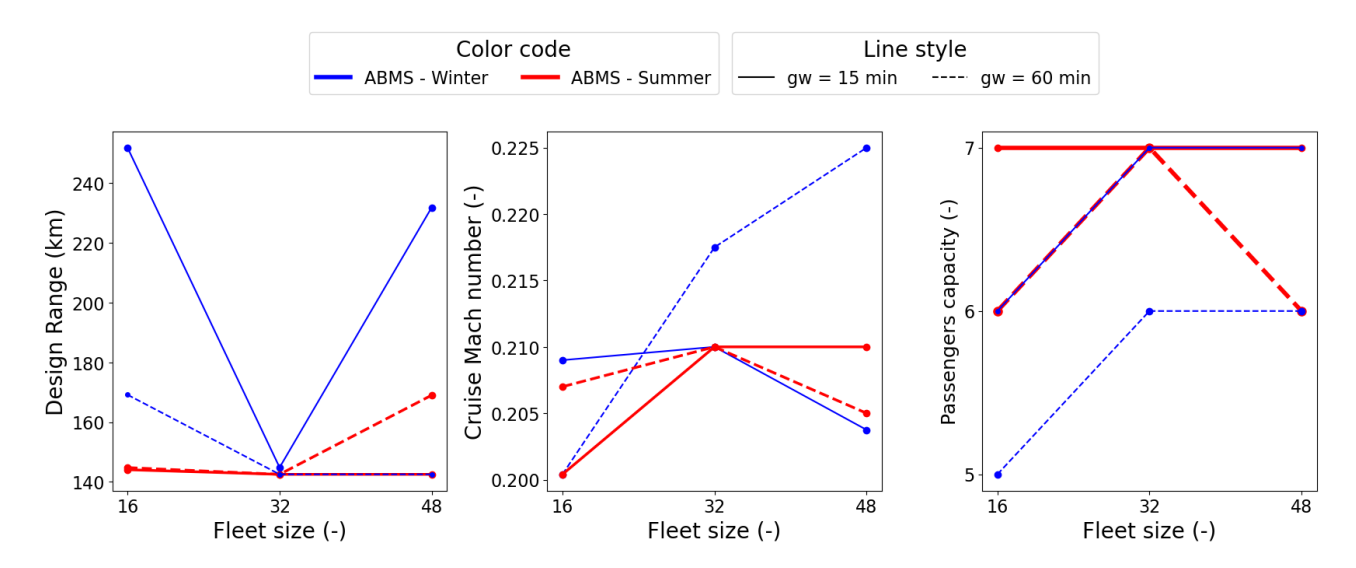


Figure 7 – Optimum seaplane design parameters in the different scenarios

# 4.3 Impact of seaplanes on the Greek maritime transportation system

In an attempt to assess the effect of adding seaplanes into the Greek maritime transport system, we look at two main indicators: service quality and sustainability. The service quality is measured in terms of the frequency and duration (travel time) of the connections. The sustainability aspect refers to both environmental sustainability, assessed considering the specific fuel consumption of the vehicles, and economic sustainability, evaluated on the basis of the average load of the vehicles.

Note that in all scenarios, seaplanes operate in addition to the ferry fleet introduced earlier, which schedule is fixed over the different scenarios. The results of each simulation are compared to a baseline scenario (representing the current status of the Greek maritime transportation system) in which the ferry fleet alone operates.

Fig. 9 depicts the variation in average service frequency caused by the operation of the different seaplane fleets. The ferry fleet's average frequency is approximately 4 (baseline), meaning that each route is connected on average twice in both directions every day (including direct and stop-over connections).

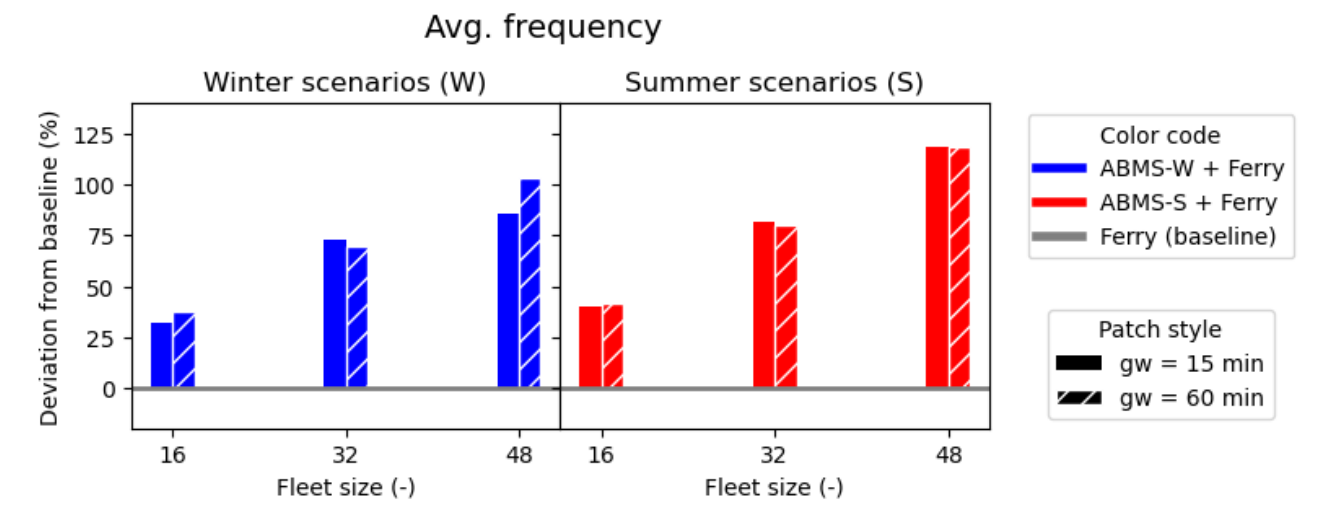


Figure 8 – Average service frequency in the different scenarios as percentage variation from the baseline

In winter scenarios, the average frequency of fleets of 16 aircraft is less than a half of the ferry fleet. Therefore, in these scenarios, not all islands are connected by seaplanes, and the overall system sees a minimum increase in average frequency of roughly 30-35%. With increasing fleet size, the average frequency of the system increases until a peak of around twice the ferries alone for  $g_W = 60 \,\mathrm{min}$ . The high grouping window has a positive effect on the service frequency in two out of the three fleet configurations. The same considerations regarding fleet size are valid for summer scenarios, while the effect of the grouping time window is less relevant in this case. Comparing winter and summer scenarios, the frequency of the connection sees a slight increase in summer with the increased demands. For both demands configurations fleet size 32 seems to be once again a critical point in which the dependency on the grouping window changes.

In Fig. 9, the relative change in average travel time is represented. In winter scenarios, the decrease in average travel time grows with fleet size, as more and more passengers can benefit of the faster seaplane service. Regarding the dependency of average travel time on the grouping time window,  $gw = 15 \, \text{min}$  allows for faster connections in all cases. The same considerations apply for summer scenarios, where however, the average connections are overall slower. This is due to the high volume of passengers. In fact, in summer scenarios, the seaplane fleets serve lower percentages of passengers with respect to the corresponding winter scenarios, therefore the impact of the faster seaplane connections is less significant on the overall average travel time. In all scenarios, seaplanes provide time savings due to the high discrepancy in speed between the two means of transportation, and secondly to the lack of direct ferry connections for some routes. Noteworthy the fact that the travel time considered for seaplanes also includes waiting time: from the moment the travel is requested until the flight departs.

The same service quality indicators can be visualized in Fig. 10, where all daily ferry connections, as well as seaplane trips for two representative scenarios are tracked on maps. This representation not only gives a strong visual impact of the differences that could be only inferred above between ferries and seaplanes speed and frequency, it also provides further insight into the network connectivity in different scenarios. Firstly, the colored lines clearly mark the difference in travel time between the two vehicles. In addition, the line thickness distribution over the different routes shows that the ferry service is quite homogeneously spread across the map, while the seaplanes focus on the most popular routes, providing much higher frequency when needed. Secondly, when looking at the overall network drawn on each map, it appears that some islands are not covered by the ferry service. In fact, seaplanes increase connectivity allowing to reach all islands in the network. Moreover, it is possible to notice that with a small seaplane fleet, the focus is on improving slower ferry routes, leaving out those connections where ferries perform at their best. With larger fleets, seaplanes start taking over more and more routes, starting from the slower ones, showing the efficiency of an on demand system.

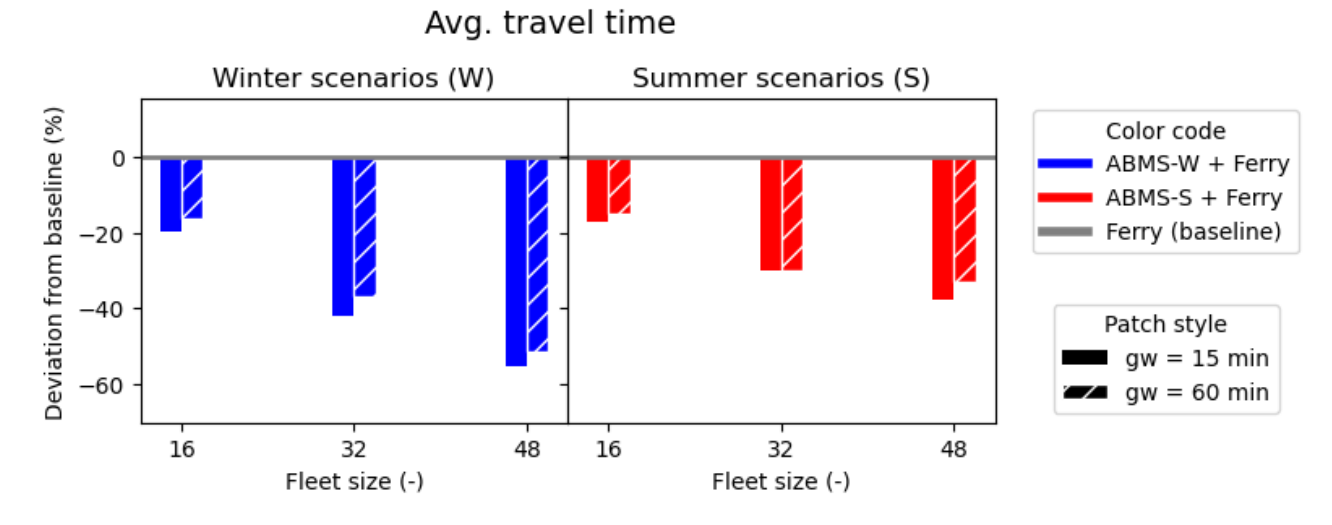


Figure 9 – Average travel time in the different scenarios as percentage variation from the baseline

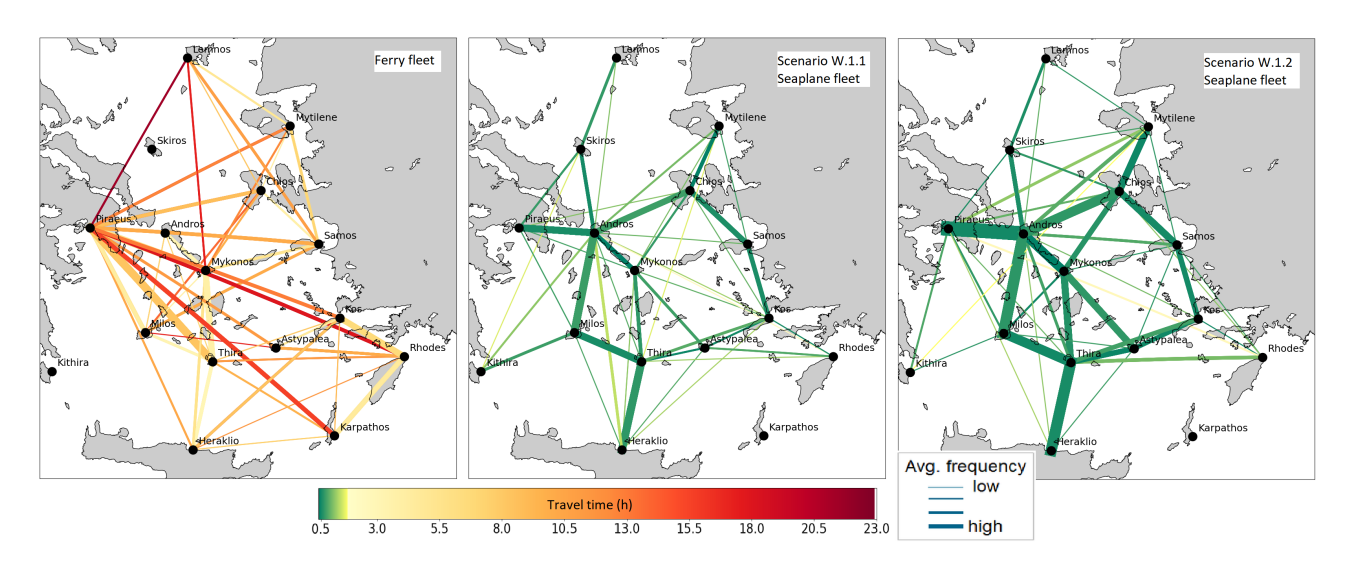


Figure 10 – Comparison of seaplanes and ferries service quality in two example scenarios

At last, the sustainability aspect is discussed for the various scenarios. In addition to the deviation of average load factor and travel time in the transport system from the baseline values, the deviation of the same metrics applied to seaplanes only (within each scenario) are also represented. The latter allows to visualize the difference between the two means of transportation in addition to the overall effect of adding seaplanes into the transport system.

In Fig. 11, the average load factor indicates the average number of passengers on board a vehicle with respect to the total capacity. In winter scenarios, the average load factor of all vehicles in the transport system decreases with respect to the baseline due to the addition of the seaplanes. In other words, for a fixed amount of travelers, introducing more vehicles in the system results in a lower average load factor. This is also evident when looking at the dependency of this parameter on the fleet size. Contrary, the average load factor of the seaplanes alone is always higher (between circa 10 and 14 times) than the baseline (ferries), indicating higher potential for covering operator costs and generating revenue. This value does not significantly change with fleet size, while its dependency from the grouping window is more evident. The higher  $g_W$  provides higher load factors.

In summer scenarios, similar trends can be observed on the overall transport system performance. However, the average load factor of seaplanes alone decreases with fleet size. In these high demand volume scenarios, when increasing fleet size, the number of mission flown is increasing at an higher rate than the requests converted, causing a decline in the seaplanes average load factors.

Moving onto Fig. 12, the specific fuel consumption is defined as mass of fuel consumed per pas-

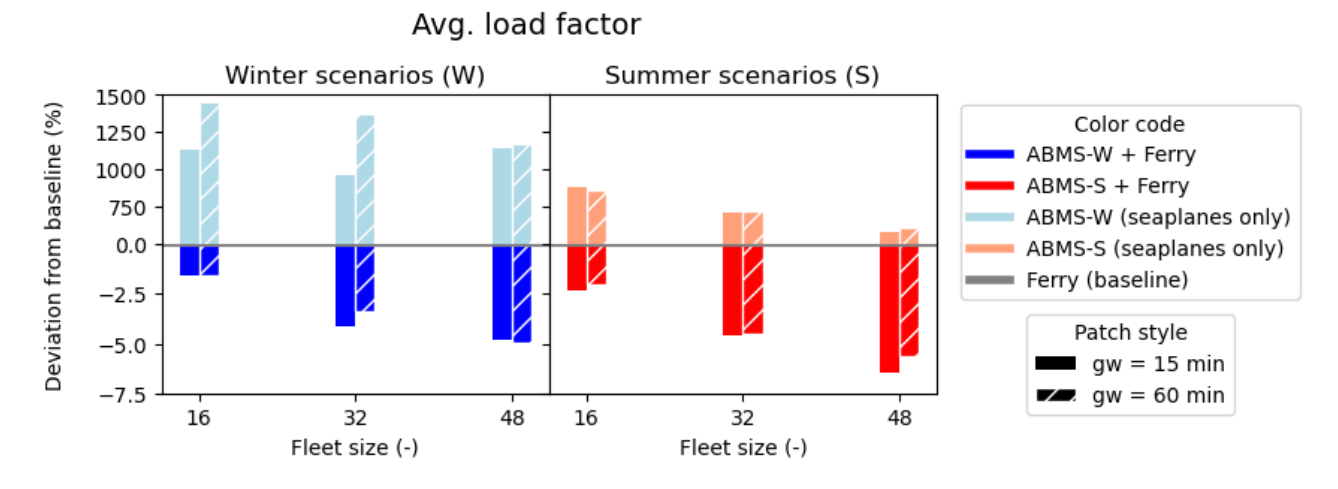


Figure 11 – Average load factor in the different scenarios as percentage variation from the baseline

senger transported. In winter scenarios, specific fuel consumption in the transport system grows with seaplane fleet size: as expected, when increasing the number of vehicles, the total fuel burnt increases (while the number of travellers per day stays the same). The higher gw provides limited fuel savings, with maximum effect for fleet size 48. The specific fuel consumption of the seaplanes is much lower than those of ferries thanks to the hybrid electric powertrain and to the high load factors, once again proving the superiority of this mean of transportation. Despite the fact that total fleet fuel consumption grows with larger fleet size, the seaplanes specific fuel consumption stays approximately constant. This is because larger fleets can also transport more passengers.

In summer scenarios, the same considerations apply, with two main differences: the effect of the grouping time window is tamed, and the performance of seaplanes alone slightly worsen with fleet size. The latter is due to the correlation of this parameter to the average load factor and the request converted.

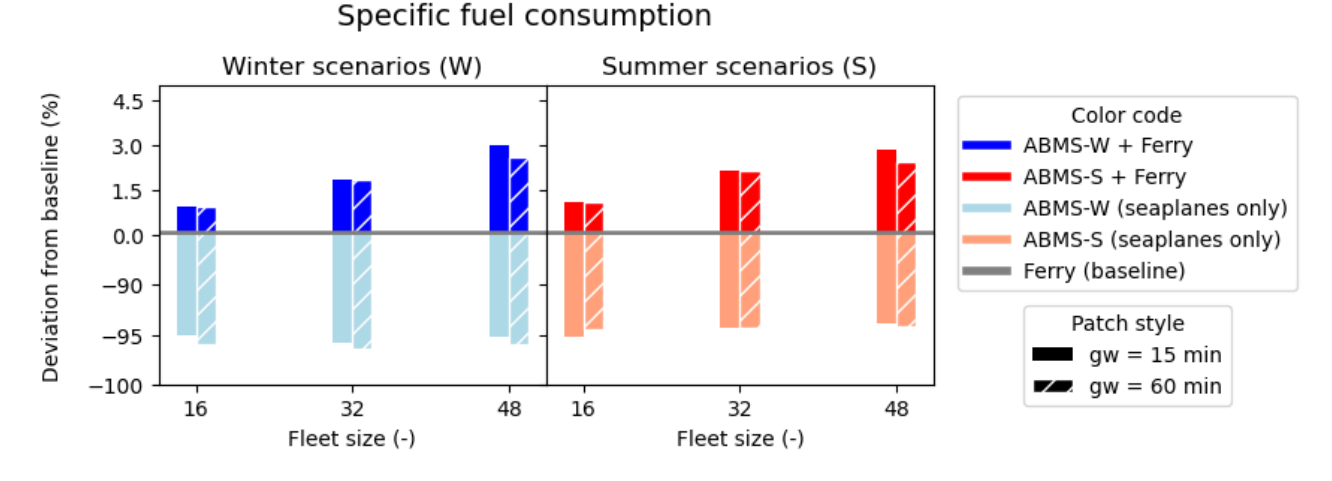


Figure 12 – Specific fuel consumption in the different scenarios as percentage variation from the baseline

#### 5 Conclusion

In conclusion, the SoS-driven aircraft design framework paves the way for new possibilities and insights in the discipline of aircraft design. For the first time, considerations about operational aspects are introduced in a methodical way in the aircraft design process, by combining a set of design tools with ABMS.

The designs outputted by the optimization appear different from expectations set by experience and conventional design approaches, as highlighted in Section 4.1. The framework demonstration

showed the effects of adding ABMS to an aircraft design framework, and the potential this methodology holds in guiding the designer in the choice of the TLARs.

The study presented in Section 4.2 unveils trends and dependencies that can help improve the operational effectiveness of conceptual designs. It emerged that the dependency of the optimum TLARs on scenario parameters weakens with growing demand volume. In other words, the optimum seaplanes across the different scenarios look more similar to each other with growing demands.

Moreover, seaplanes proved to be a valid addition to maritime connections in the Greek islands, providing relevant time savings, and increasing the frequency of connections as seen in Section 4.3. The research also revealed that these benefits come with a considerably small increase in fuel consumption, and thus emissions, when operating hybrid electric seaplanes. Moreover, the average load factor of the vehicles shows that seaplanes also offer promising advantages from a business perspective as they operate closer to their maximum capacity than ferries do.

In summary, from an aircraft design point of view, this work shows that including a SoS analysis in the aircraft conceptual design stage is beneficial for the realization of more efficient concepts. From an operational point of view, the results suggest that a hybrid electric seaplane fleet of approximately 32 aircraft could replace large part of the ferry fleet considered. In such a scenario, seaplanes could accommodate approximately 40% of summer travel demands while reducing average travel time over 30% and fuel consumption per passenger transported by circa 90%.

The significant disparity emerged from this study between ferries and seaplanes seeds doubts about the fairness of the comparison between seaplanes sized for an on-demand transport system and a ferry fleet thought for a scheduled transportation system. Future work will need to focus on clarifying this aspect, by proposing a different comparison and metrics of evaluation, and above all, exploring different assumptions regarding the ferry schedule, and their passenger capacity. In addition, regarding the dependency identified between the optimum seaplane design parameters and scenario uncertainty parameters, the conclusions could be strengthened by broadening the analysis, performing simulations in an higher number of scenarios, and in particular for more fleet sizes and demand volumes.

## 6 Contact Author Email Address

Mailto: vincenzo.nugnes@dlr.de

# 7 Acknowledgements

The authors thank Nazlican Cigal and Hussain Nabih Naeem for their guidance and support on the topic of ABM and for introducing the SoSID Toolkit, which was instrumental in this research project. The research presented in this paper has been performed in the framework of the COLOSSUS project (Collaborative System of Systems Exploration of Aviation Products, Services and Business Models [36]) and has received funding from the European Union Horizon Europe program under grant agreement No. 101097120.

## 8 Copyright Statement

The authors confirm that they, and/or their company or organization, hold copyright on all of the original material included in this paper. The authors also confirm that they have obtained permission, from the copyright holder of any third-party material included in this paper, to publish it as part of their paper. The authors confirm that they give permission, or have obtained permission from the copyright holder of this paper, for the publication and distribution of this paper as part of the ICAS proceedings or as individual off-prints from the proceedings.

#### References

- [1] Michael Schmidt, Annika Paul, Mara Cole, and Kay Olaf Ploetner. Challenges for ground operations arising from aircraft concepts using alternative energy. *Journal of Air Transport Management*, 56:107–117, 2016.
- [2] Prajwal Shiva Prakasha, Nabih Naeem, Patrick Ratei, and Björn Nagel. Aircraft architecture and fleet assessment framework for urban air mobility using a system of systems approach. *Aerospace Science and Technology*, 2021.

- [3] Liu Hu, Tian Yongliang, Gao Yuan, Bai Jinpeng, and Zheng Jiangan. System of systems oriented flight vehicle conceptual design: Perspectives and progresses. *Chinese Journal of Aeronautics*, 28(3):617–635, 2015.
- [4] ISO, IEC, and IEEE 21839. Iso/iec/ieee international standard systems and software engineering system of systems (sos) considerations in life cycle stages of a system. ISO/IEC/IEEE 21839:2019(E), pages 1–40, 2019.
- [5] Mo Jamshidi. System of systems engineering a definition. *Piscataway, NJ: IEEE SMC*, 2005.
- [6] Dan Delaurentis. Understanding transportation as system-of-systems design problem. *AIAA Aerospace Sciences Meeting and Exhibit, Reno, Nevada*, January 2005.
- [7] Daniel Delaurentis, Kushal Moolchandani, and Cesare Guariniello. *System of Systems Modeling and Analysis*, chapter 3,4,6. Taylor and Francis Group, 2023.
- [8] Soufiane Bouarfa, H.A.P. Blom, Alexei Sharpanskykh, and K Belhadji. Agent-based modelling and simulation of airline operations control decision-making under uncertainty. *AIAA Scitech 2021 Forum*, 2021.
- [9] Gianfranco La Rocca. Seaplanes and amphibians. Encyclopedia of Aerospace Engineering, 2010.
- [10] Errikos Levis. Design synthesis of advanced technology, flying wing seaplanes. Technical report, Imperial College of Science, Technology and Medicine, London, 2012.
- [11] Alan Canamar. Seaplane conceptual design and sizing. Technical report, University of Glasgow, 2012.
- [12] Jason W. Cary and Gilbert L. Crouse. Preliminary design optimization of an amphibious aircraft. *AIAA Aerospace Sciences Meeting*, 2012.
- [13] Sebastian Wöhler, Georgi Atanasov, Daniel Silberhorn, Benjamin Fröhler, and Thomas Zill. Preliminary aircraft design within a multidisciplinary and multifidelity design environment. *Aerospace Europe Conference 2020*, 2020.
- [14] E. J. Alvarez, J. Mehr, and A. Ning. Flowunsteady: An interactional aerodynamics solver for multirotor aircraft and wind energy. *AIAA AVIATION 2022 Forum*, 2022.
- [15] M. Fouda, E. J. Adler, J. H. Bussemaker, J. R. A. Martins, D. F. Kurtulus, L. Boggero, and B. Nagel. Automated hybrid propulsion model construction for conceptual aircraft design and optimization. *Congress of the International Council of the Aeronautical Sciences (ICAS 2022)*, 2022.
- [16] Benjamin J. Brelje and Joaquim R. R. A. Martins. Development of a conceptual design model for aircraft electric propulsion with efficient gradients. In *2018 AIAA/IEEE Electric Aircraft Technologies Symposium*, Cincinnati, OH, July 2018.
- [17] Jasper Bussemaker, Raúl García Sánchez, Mahmoud Fouda, Luca Boggero, and Björn Nagel. Function-based architecture optimization: An application to hybrid-electric propulsion systems. *INCOSE international symposium*, 2023.
- [18] San Kilkis, Prajwal S. Prakasha, Nabih Naeem, and Björn Nagel. A python modelling and simulation toolkit for rapid development of system of systems inverse design (sosid) case studies. *AIAA AVIATION 2021 FORUM*, 2021.
- [19] Brigitte Boden, Jan Flink, Robert Mischke Niklas Först, Kathrin Schaffert, Alexander Weinert, Annika Wohlan, and Andreas Schreiber. Rce: an integration environment for engineering and science. *SoftwareX* 15, 2021.
- [20] M. Alder, E. Moerland, J. Jepsen, and B. Nagel. Recent advances in establishing a common language for aircraft design with cpacs. *Aerospace Europe Conference 2020*, 2020.
- [21] Sébastien Le Digabel. Algorithm 909: Nomad: Nonlinear optimization with the mads algorithm. *ACM Trans. Math. Softw.*, 37(4), feb 2011.
- [22] D. P. Raymer. Aircraft Design: A Conceptual Approach, Second Edition. AIAA Education Series, 1992.
- [23] Yann Fefermann, Christophe Maury, Clélia Level, Khaled Zarati, Jean-Philippe Salanne, Clément Pornet, Bruno Thoraval, and Askin T. Isikveren. Hybrid-electric motive power systems for commuter transport applications. 30th congress of the International Council of the Aeronautical Sciences (ICAS), 2016.
- [24] Annegret Stephan, Tim Hettesheimer, Christoph Neef, Thomas Schmaltz, Steffen Link, Maximilian Stephan, Jan Luca Heizmann, and Axel Thielmann. Alternative battery technologies roadmap 2030+. Fraunhofer Institute, 9 2023.
- [25] Benjamin J. Brelje and Joaquim R.R.A. Martins. Electric, hybrid, and turboelectric fixed-wing aircraft: A review of concepts, models, and design approaches. *Progress in Aerospace Sciences*, 104:1–19, 3 2019
- [26] Peter Stenzel, Manuel Baumann, Johannes Fleer, Benedikt Zimmermann, and Marcel Weil. Database development and evaluation for techno-economic assessments of electrochemical energy storage systems. IEEE, 5 2014.
- [27] Stamatios Ntanos. Energy consumption and carbon dioxide emissions of a suburban coastal transport

- system. 05 2008.
- [28] Ilopoulou, Kepaptsoglou, and Karlafitis. Route planning for a seaplane service: The case of the greek islands. *Computers and Operations Research*, 59:66–77, 2015.
- [29] Tie-Qiao Tang, Shao-Peng Yang, Hui Ou, Liang Chen, and Hai-Jun Huang. An aircraft boarding model with the group behavior and the quantity of luggage. *Transportation Research Part C: Emerging Technologies*, 93:115–127, 2018.
- [30] Michael Schmidt. A review of aircraft turnaround operations and simulations. *Progress in Aerospace Sciences*, 92:25–38, 2017.
- [31] Anna Tomaszewska, Zhengyu Chu, Xuning Feng, Simon O'Kane, Xinhua Liu, Jingyi Chen, Chenzhen Ji, Elizabeth Endler, Ruihe Li, Lishuo Liu, Yalun Li, Siqi Zheng, Sebastian Vetterlein, Ming Gao, Jiuyu Du, Michael Parkes, Minggao Ouyang, Monica Marinescu, Gregory Offer, and Billy Wu. Lithium-ion battery fast charging: A review. *eTransportation*, 1:100011, 2019.
- [32] Upendra Rohatgi. Sizing of an aircraft fuel pump. International Journal of Multiphase Flow INT J MULTIPHASE FLOW, 22, 12 1996.
- [33] L. Minghui, F. Xiong, W. Zhendong, Y. Wen, and Z. Weijing. Modification design of aircraft ground pressure refueling system. In *CSAA/IET International Conference on Aircraft Utility Systems (AUS 2020)*, volume 2020, pages 863–868, 2020.
- [34] Menno Berger. A door-to-door multimodal simulation-based framework for the integration of advanced air mobility design and operations. DLR-Interner Bericht. DLR-IB-SL-HF-2023-159. Master's. Delft University of Technology., 2023.
- [35] Michael D. Patterson, Kevin R. Antcliff, and Lee W. Kohlman. A proposed approach to studying urban air mobility missions including an initial exploration of mission requirements. *AHS International 74th Annual Forum I& Technology Display*, 5 2018.
- [36] Prajwal Shiva Prakasha et al. Colossus eu project collaborative system of systems exploration of aviation products, services and business models: Overview and approach. *ICAS*, 2024.